Supplementary Information

Molecular mechanisms of aberrant neutrophil differentiation in glycogen storage disease type Ib

Cellular and Molecular Life Sciences

Sang Wan Sim[1], Yuyeon Jang[1], Tae Sub Park[2], Byung-Chul Park[2], Young Mok Lee[3*], Hyun Sik Jun[1*]

* Hyun Sik Jun is a lead author between the two corresponding authors.

Correspondence should be addressed to:

Young Mok Lee

Department of Pediatrics, University of Connecticut School of Medicine

Farmington CT 06030, USA

E-mail: yolee@uchc.edu

Hyun Sik Jun

Department of Biotechnology and Bioinformatics, College of Science and Technology, Korea University, Sejong 339-700, Republic of Korea

E-mail: toddjun@korea.ac.kr

Supplementary material and methods

Establishment of Cas9-mediated G6PT$^{-/-}$ HL-60

For knockout of the human *G6PT* gene in HL-60s, Cas9 endonuclease target loci were designed in exon 5 of the human *G6PT* gene (Fig. S2a). A single gRNA was designed with 20 bp target sequence followed by protospacer adjacent motif (PAM) sequences (Fig. S2a). Co-transfection, sorting, genotyping, and sequencing were performed as described previously [1]. Potential off-target sites were identified using TagScan (http://www.isrec.isb-sib.ch/tagger), a web tool providing genome searches for short sequences, followed by PCR and sequencing. G6PT expression level decreased to 13.7% in *G6PT*$^{-/-}$ HL-60s, as compared to that in the control HL-60s (Fig. S2b). To exclude potential off-target effects by gRNA, ten putative off-target sites were identified and sequenced (data not shown). No mutations were detected in any of the sites of *G6PT*$^{-/-}$ HL-60s. The morphology of *G6PT*$^{-/-}$ HL-60s cells was analyzed using flow cytometry. There was an increase in the cell size (forward scatter) in the *G6PT*$^{-/-}$ HL-60s, as compared to that in the control HL-60s, while cell granularity (side scatter) was not different between both the groups (Fig. S2c).

Annexin V binding assay

Apoptosis of differentiated HL-60s (dHL-60s) was examined by flow cytometry using the annexin V-fluorescein isothiocyanate (FITC, Santa Cruz Biotechnology) and propidium iodide (PI) as described previously [2]. dHL-60s were incubated with annexin V-FITC and propidium iodide (PI) for 15 minutes. Flow cytometry was performed using a Guava® EasyCyte™ system (Millipore) and the data were analyzed using FlowJo v7.0.

Supplementary figure legends

Fig. S1 Expression of granulocyte-colony stimulating factor receptor (G-CSFR) and C-X-C chemokine receptor type 4 (CXCR4) in the blood and bone marrow of *G6pt*$^{-/-}$ mice. **a** Representative flow cytometric analysis of blood neutrophils and their G-CSFR and CXCR4 expression. **b** Representative flow cytometry data of neutrophil lineage cells and their expression of G-CSFR and CXCR4 in the bone marrow.

Fig. S2 Targeting of the G6PT using CRISPR/Cas9 and phenotypes of *G6PT*$^{-/-}$ HL-60s. **a** Genomic sequence and structure of the human *G6PT* gene. Lowercase and capital letters indicate the intron and exon sequences, respectively. Guide RNA (gRNA) targeting sites (red capital letters) are shown with a protospacer adjacent motif sequence in bold. Deleted nucleotides are underlined. **b** mRNA levels of G6PT in control and *G6PT*$^{-/-}$ HL-60s. **c** Representative images and mean FSC and SSC. **d-e** Representative flow cytometry analysis of neutrophil differentiation markers, CD38 and CD11b, at the indicated time. Data represent the mean ± SEM (n=3). *$p < 0.05$, **$p < 0.01$.

Fig. S3 Apoptosis of control and *G6PT*$^{-/-}$ HL-60s during neutrophil differentiation. **a** Representative flow cytometry analysis of annexin V binding and PI uptake at the indicated time. **b** Protein levels of full length and cleaved poly (ADP-ribose) polymerase (PARP).

Fig. S4 Neutrophil differentiation of control and *G6PT*$^{-/-}$ HL-60s depending on the glucose. **a** Growth curve of control (a) and *G6PT*$^{-/-}$ HL-60s (b) depending on the glucose concentration at the indicated time in the presence of dimethyl sulfoxide (DMSO) and all-trans retinoic acid (ATRA) **c** Mean fluorescence intensity (MFI) of CD38 expression and frequency of CD11b^{+} cells at 96 h after induction. **d** Representative Hema-3-stained cytospins of DMSO and ATRA-induced control and *G6PT*$^{-/-}$ HL-60s

depending on the glucose concentration at 96 h after induction (bar = 10 μm). **e** Growth curve of control and *G6PT*$^{-/-}$ HL-60s in the presence of 0.5 mM 2-deoxy-D-glucose (2-DG) after induction. **f** MFI of CD38 and frequency of CD11b^{+} cells at 96 h after induction in the indicated condition. **g** Representative Hema-3-stained cytospins of differentiated HL-60s in the indicated condition (bar = 10 μm). Data represent the mean ± SEM (n = 3). *$p < 0.05$, ** $P < 0.01$.

Fig. S5 Decreased nuclear localization of PPARγ in *G6PT*$^{-/-}$ HL-60s. **a** Quantification of the integrated fluorescence intensity by imageJ. Data represent the mean ± SEM (n = 3). *$p < 0.05$, ** $P < 0.01$.

Supplementary table 1 List of specific primers used in the present study

Gene		5' to 3' sequence	Tm (℃)	Amplicon size (bp)
18S rRNA	Forward	GGC CCT GTA ATT GGA ATG AGT C	56.8	146
	Reverse	CCA AGA TCC AAC TAC GAG CTT	55.3	
p21	Forward	AGG GGA CAG CAG AGG AAG	58.1	158
	Reverse	GCG TTT GGA GTG GTA GAA ATC TG	56.9	
CD36	Forward	GAG AAC TGT TAT GGG GCT AT	52	389
	Reverse	TTC AAC TGG AGA GGC AAA GG	55.9	
ABCG1	Forward	GAC CTT TCC TAT TCG GTT CCT G	56.2	104
	Reverse	GCC ACC AAC TCA CCA CTA TT	56	
ACOT2	Forward	CTG TGA TGG CTC TGG CTT ATT A	55.1	107
	Reverse	GGG ATG ACT GAG CAA GTA GTT C	56.1	

* TaqMan probe used in this study was SLC37A4, HS00894592_g1.

* BioRad Prime PCR Primers (SYBR green primer) used in this study were PPARα, qHsaCID0011001; PPARγ, qHsaCID0011718.

References

1. Jeon EH, Park TS, Jang Y, Hwang E, Kim SJ, Song KD, Weinstein DA, Lee YM, Park BC, Jun HS (2020) Glucose-6-phosphate transporter mediates macrophage proliferation and functions by regulating glycolysis and mitochondrial respiration. Biochem Biophys Res Commun 524:89-95. https://doi.org/10.1016/j.bbrc.2020.01.043
2. Kim SY, Jun HS, Mead PA, Mansfield BC, Chou JY (2008) Neutrophil stress and apoptosis underlie myeloid dysfunction in glycogen storage disease type Ib. Blood 111:5704-5711. https://doi.org/10.1182/blood-2007-12-129114

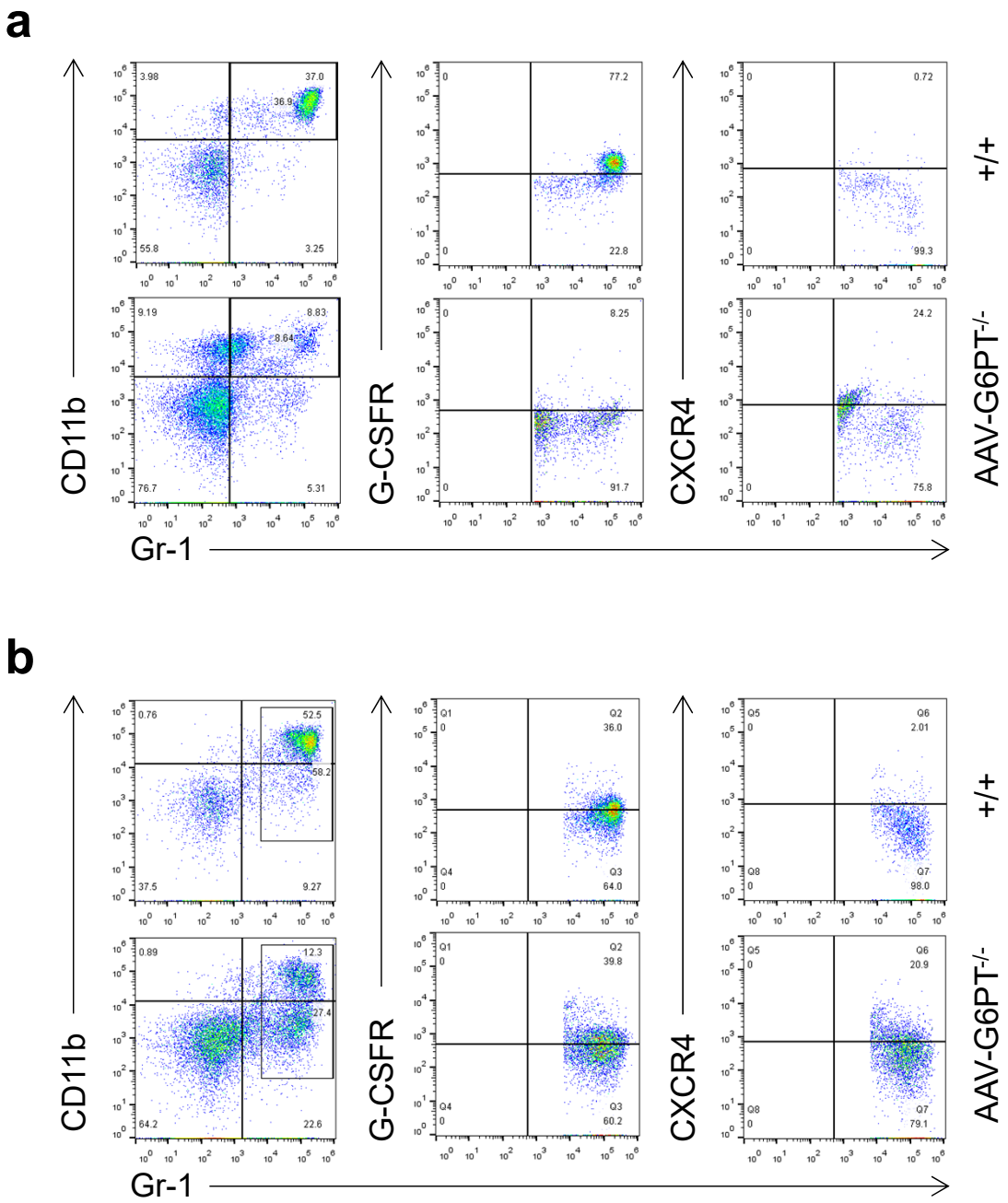

Supplementary fig. 1

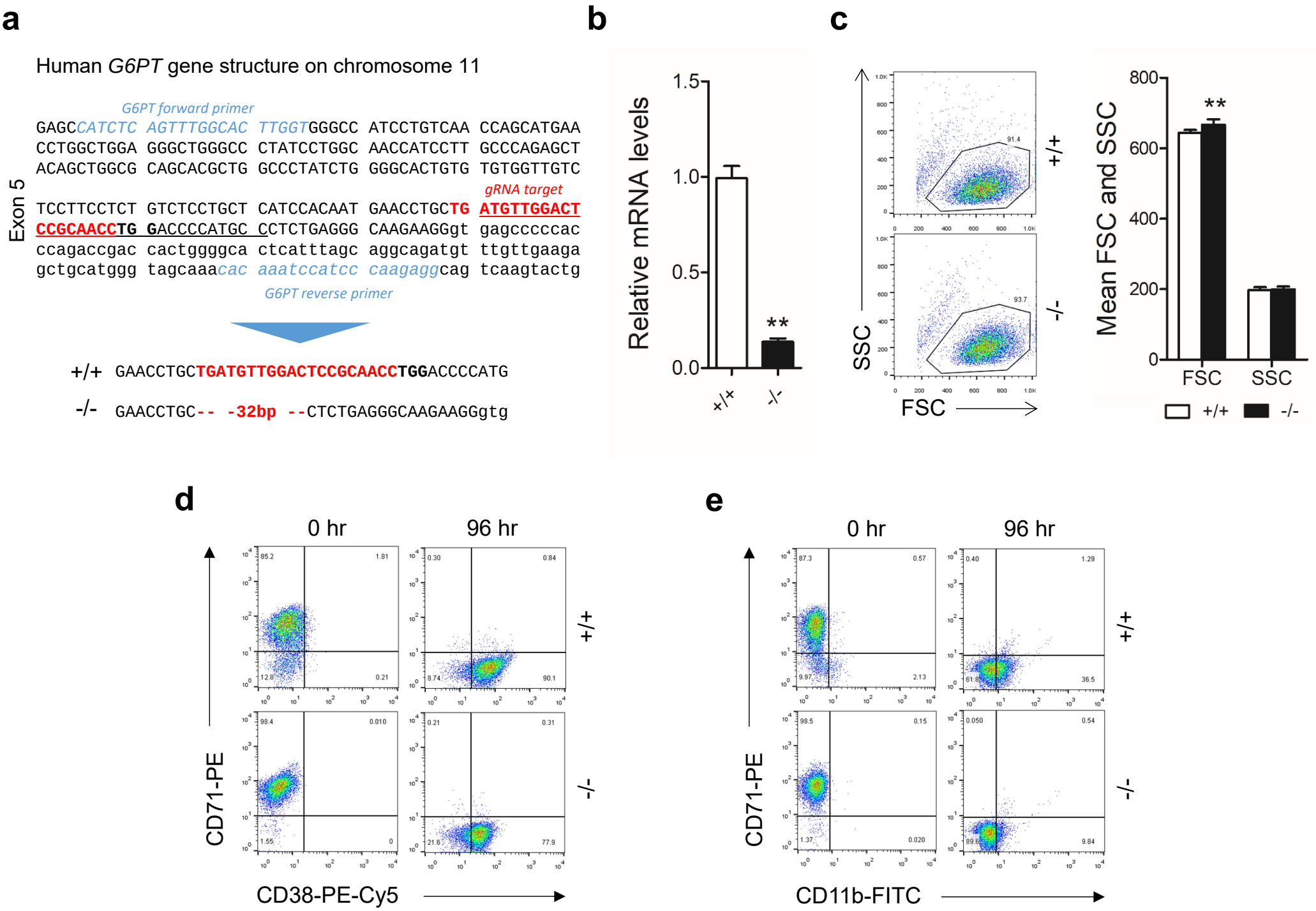

Supplementary fig. 2

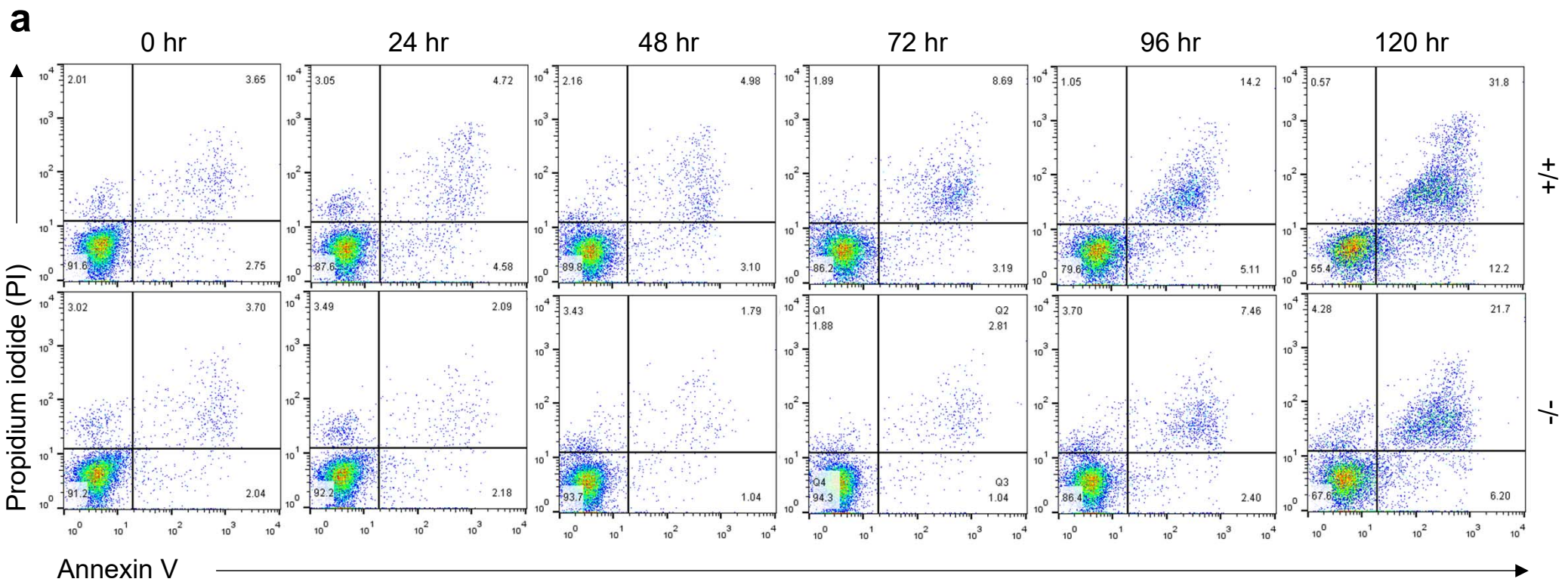

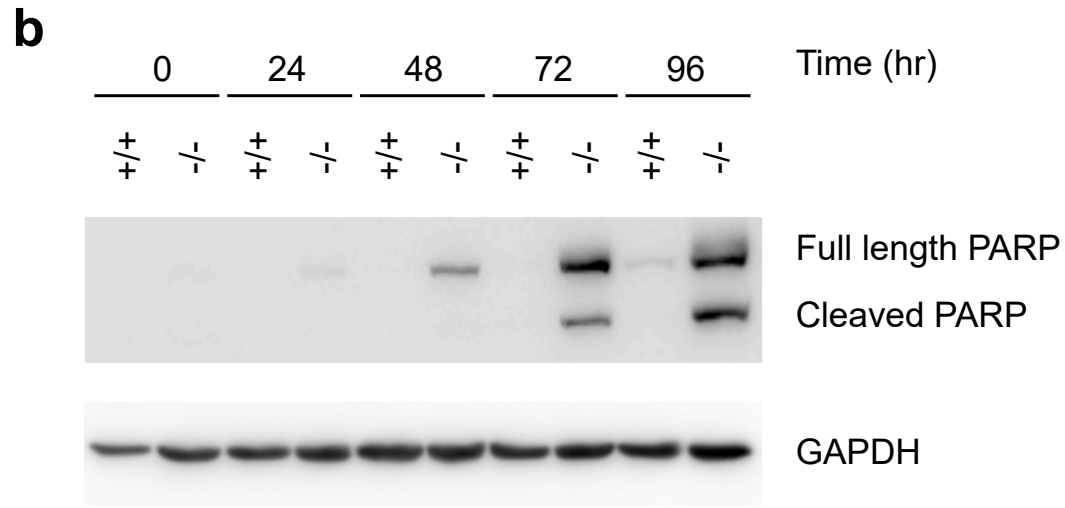

Supplementary fig. 3

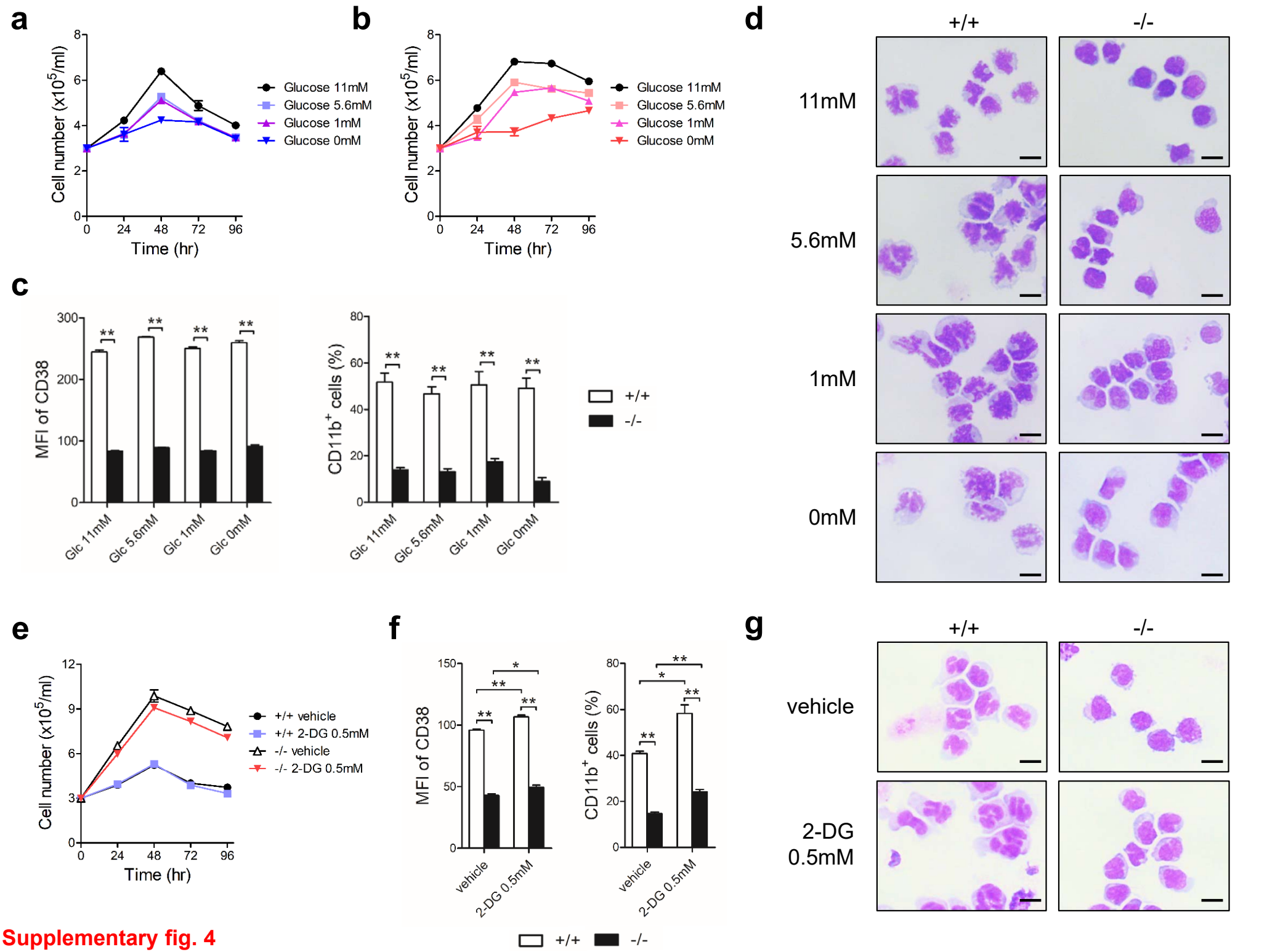

Supplementary fig. 4

a

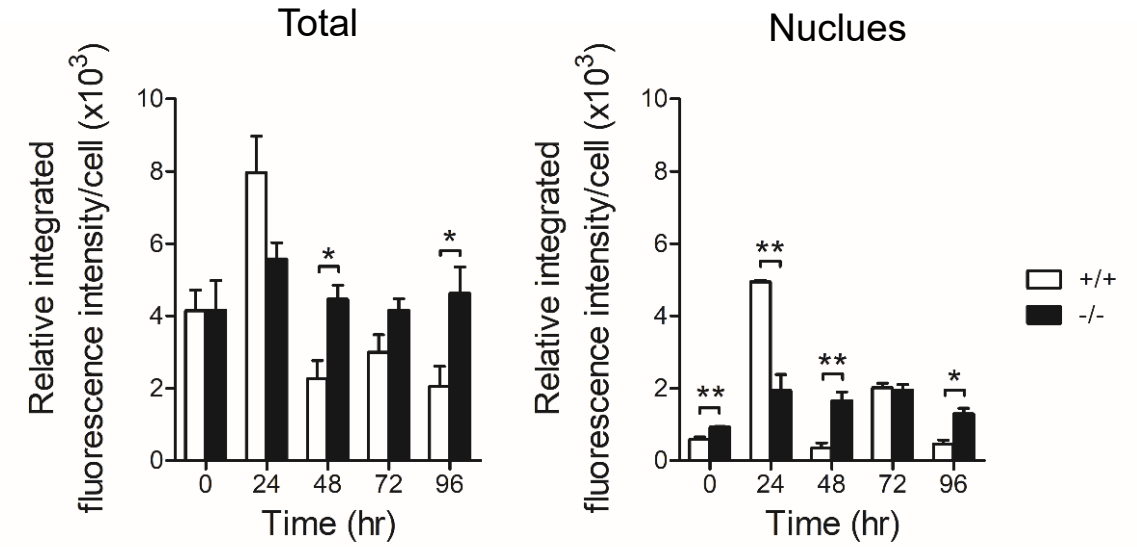

Supplementary fig. 5